Chapter 5

Pushing Limits: Fluoride Sensing in water at ppb Level using a Novel Colorimetric and Fluorometric Approach with Perylene Tetracarboxylate Dye

5.1. Introduction

Perylene is a brown solid material discovered by Kardos in 1913 [1,2]. This molecule is a planar aromatic compound containing five phenyl rings that possess strong affinity to interact with others through its π-cloud. Low solubility in common and widely-used solvents prevented the recognition of its fluorescent properties until 1959. Since then, various studies have been accomplished on perylene based material to make its derivatives in order to improve its solubility, and to be explored as pigment [3,4]. Perylene-3,4,9,10-tetracarboxylic dianhydride (PTCDA) is a widely explored perylene derivatives known for its synthetic importance and distinct electronic and photophysical properties [5,6]. PTCDA, a derivative of perylene, is characterized by the presence of two anhydride groups that offer a unique platform for chemical modifications and functionalization. This structural versatility, combined with its planar aromatic core, results in strong π-π stacking interactions, high thermal stability, and remarkable electron-accepting capabilities, making PTCDA a valuable material in various scientific and technological applications [8]. One of the significant applications of PTCDA is in the synthesis of anion and cation sensing chemosensors based on Perylene-3,4,9,10-tetracarboxylicdiimide (PTCDI), reported first in 1913 as Pigment Red 179 [9-15]. PTCDIs first reported in 1913 are known Pigment Red 179. In the realm of organic electronics, PTCDI derivatives are widely used as n-type semiconductors in organic field-effect transistors (OFETs). Their strong absorption in the visible region, high extinction coefficients, and excellent photostability enable them to function effectively as active layers in photovoltaic applications [16,17]. In recent years, PTCDI derivatives have also been explored for their potential in energy storage and conversion applications due to their excellent stability and redox-active nature [18,19]. PTCDI derivatives are also extensively studied for their applications in sensing technologies. Their strong fluorescence, high quantum yields, and excellent photostability make them ideal candidates for fluorescence-based sensors. These materials can be functionalized to detect a wide range of analytes, including metal ions, organic molecules, and biological species [9-15]. These sensors operate by exhibiting changes in their fluorescence intensity or wavelength upon binding with the target analytes, enabling sensitive and selective detection. In addition to ion sensing, PTCDI derivatives have been employed in the detection of organic molecules and biomolecules. For instance, they have been used to detect explosives, pesticides, and other hazardous chemicals [20]. These PTCDI derivatives operates based on mechanisms such as photoinduced electron transfer

(PET), charge transfer (CT), or fluorescence resonance energy transfer (FRET), which are influenced by the binding of target analytes [21-26]. The structure of some of the PTCDI based sensor probe molecules studied towards metal ion sensing are shown in figure 5.1.
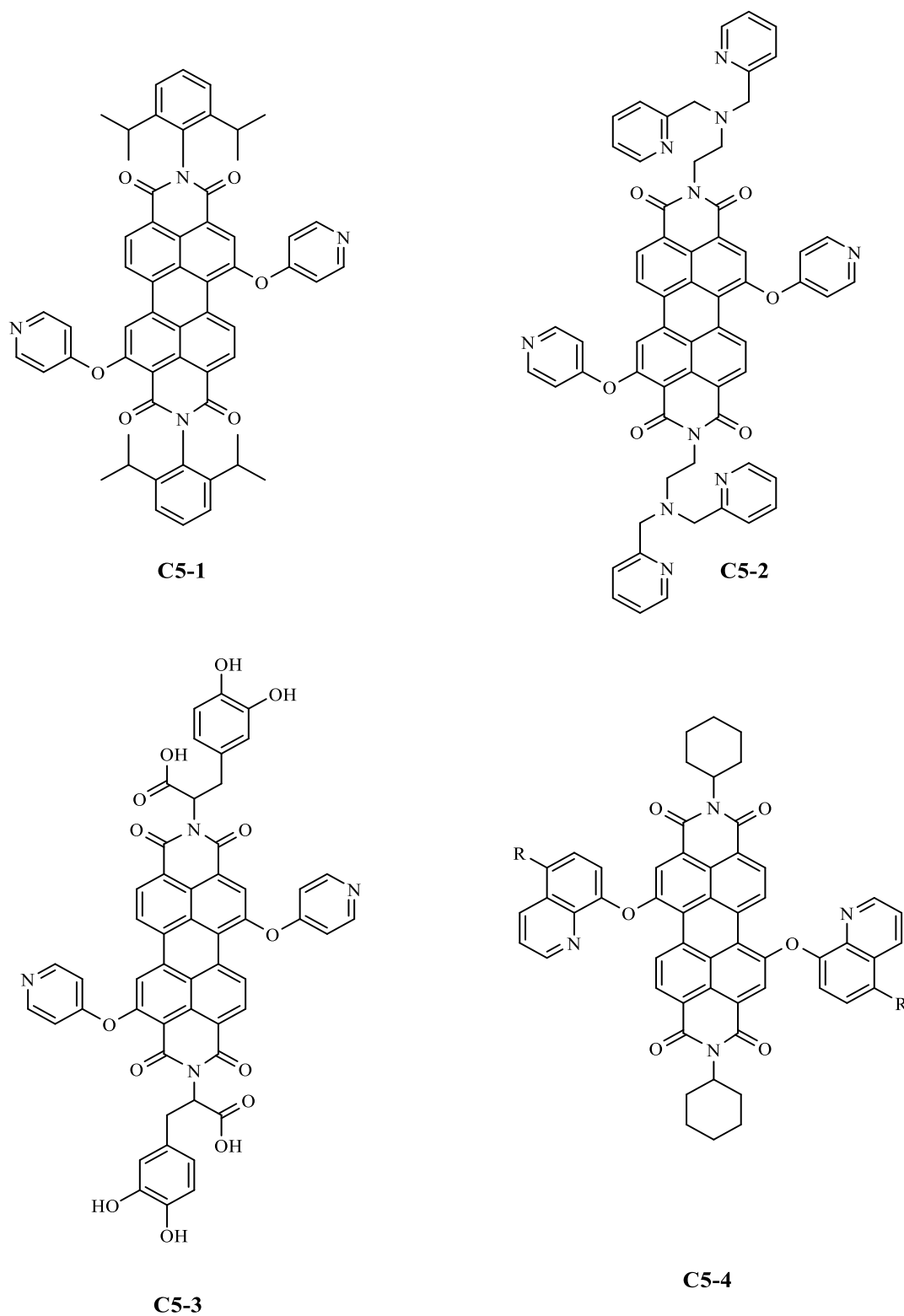

C5-1

C5-2

C5-3

C5-4

Figure 5.1: Derivatives of PTCDI used for detection of metal cation.

Generally, in the PTCDI based ion sensor, the nature of the analyte that senses depend on the nature of the recognition unit introduced in the perylenediimide periphery whereas the perylenediimide core is responsible for the reporting of the binding event through characteristic optical changes. For instance, for the purpose of recognition of anion the PTCDI is functionalised with anion binding functionality and successfully fabricated receptors for a range of anions including fluoride, acetate and phosphate ions, etc. [27]. It has been found that the fluoride sensing study reported on PTCDI derivatives are typically performed in organic media rather than pure water (Table 5.1). For instance, recently Yin *et al*. reported the synthesis of a perylenemonoimide-based colorimetric and fluorometric probe for detecting fluoride ion in presence of Ag^+ ion. Although they were successful in detecting fluoride at very low concentrations, the fluoride source used was tetrabutylammonium salt dissolved in an organic solvent (THF) [28].

 From the review of literature on perylene core based optical sensor, it is found that almost all the probe molecules studied for sensing purposes are the derivatives of PTCDI. Although PTCDI based probe depicted excellent optical response upon ion recognition but the synthesis and functionalization of PTCDI derivatives involves troublesome synthetic protocols [29,30]. On the other hand, 3,4,9,10-Perylenetetracarboxylic acid, another derivative of perylene, can be easily synthesized from the base hydrolysis of PTCDA. Moreover, the potassium salt of perylenetetracarboxylate (K_4PTC) are highly soluble in water and also exhibits excellent bright luminescence and electrochemical properties [31]. Although the application of K_4PTC as electrode materials in battery application is well documented, the work on sensor is not yet explored [32]. In 2018, Botana *et al*. demonstrated three-dimensional metal-organic framework (MOF) of K_4PTC as humidity actuators on flexible substrates with printed techniques [33]. Recently, Rajamohan and co-workers reported potassium-PTCA (K_4PTCA) based MOFs as an efficient sensing probe for Cu^{2+} and Pb^{2+} detection [34].

In the attempt to use K_4PTC as a fluoride sensor probe, herein we have demonstrated a complimentary methodology based on hypothesis 2 where fluoride recognition is achieved in an indirect way. K_4PTC was first converted to Al^{3+}-PTC complex which was subsequently used in the fluorometric/colorimetric recognition of fluoride ion in water medium. It was envisaged that fluoride is a hard base so it has the potential to take out Al^{3+} ion, (a hard acid) from the complex of Al^{3+} with a relatively softer base than fluoride (Figure 5.2).
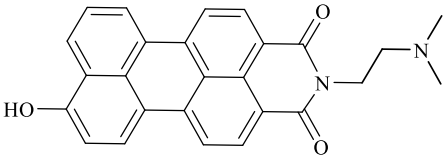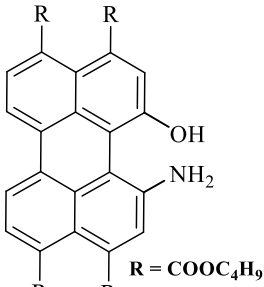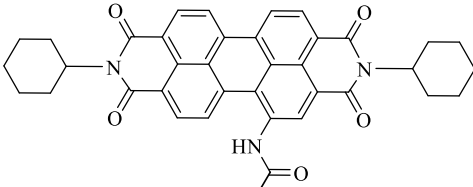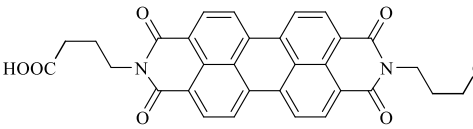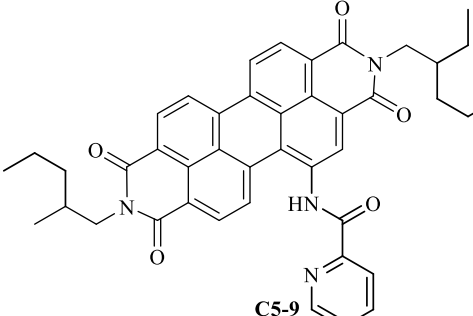
Probe	Anion(s) detected	Solvent of study	Types of sensor	References
C5-5	F^-/Ag^+	THF	Chromogenic	[35]
C5-6 R = COOC₄H₉	CN^-	DMSO	Chromogenic	[36]
C5-7	F^-	DCM	Chromogenic and fluorogenic	[37]
C5-8	F^-	DMSO/ H_2O	Chromogenic	[38]
C5-9	$F^-/Cu(II)$	THF/M OPS buffer	Chromogenic and fluorogenic	[39]

Table 5.1: Derivatives of Perylene used for detection of fluoride anion.
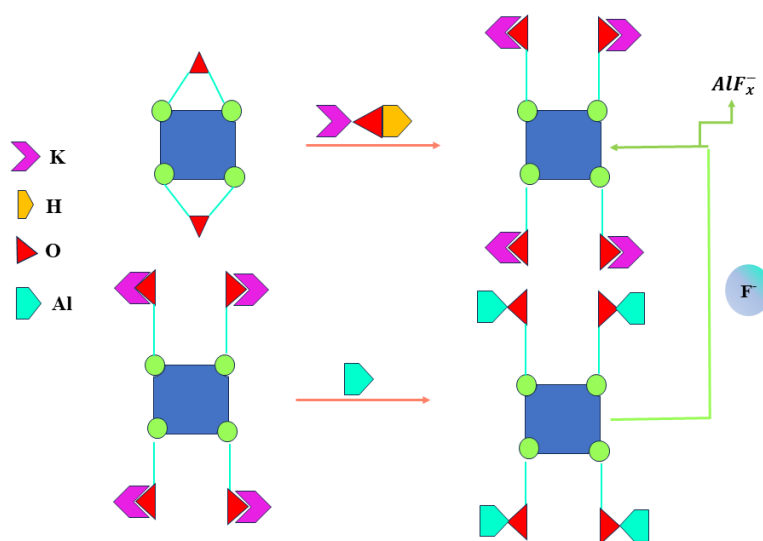
Figure 5.2: Schematic diagram of the demonstrated methodology.

5.2. Objective of the study

- To standardised a methodology for the sensing of fluoride ion with potassium salt of 3,4,9,10-Perylenetetracarboxylic acid (K$_4$PTC) in 100% water as per hypothesis 2.
- To investigate mechanism of the process.
- To validate the sensing performance of the methodology with real life sample.

5.3. General experimental details

5.3.1 Synthesis of K$_4$PTC
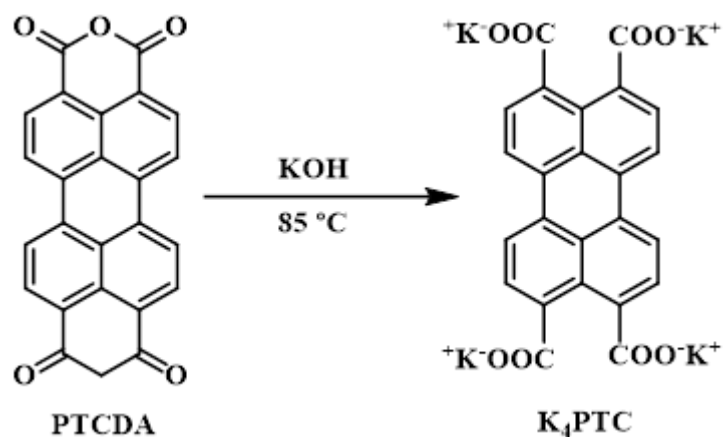
Scheme 1: Synthesis of **K$_4$PTC.**

K$_4$PTC was prepared by following literature reported method [40]. 2.25 mmol of Perylenetetracarboxylic dianhydride (PTCDA) was dissolved in 20 mL of ethanol, followed by the addition of 100 mmol of Potassium hydroxide (KOH) with continuous stirring. The initially reddish-brown solution transformed into a highly intense greenish-yellow solution as the sparingly soluble PTCDA completely dissolved. Subsequently, the solution was heated to 80° - 90° C for 8h and then allowed to cool. After cooling, water was gradually added to the reaction mixture until a complete precipitation of yellow crude solid (potassium salt of PTC) was obtained. The product was further crystallized from hot water as orange crystals. Comparison of the PXRD of the synthesized MOF with the simulated PXRD from the single crystal XRD data obtained from the Cambridge Crystallographic Data Centre (CCDC numbers is 1509483) revealed the formation of the K$_4$PTC MOF (Figure 5.3) [33].
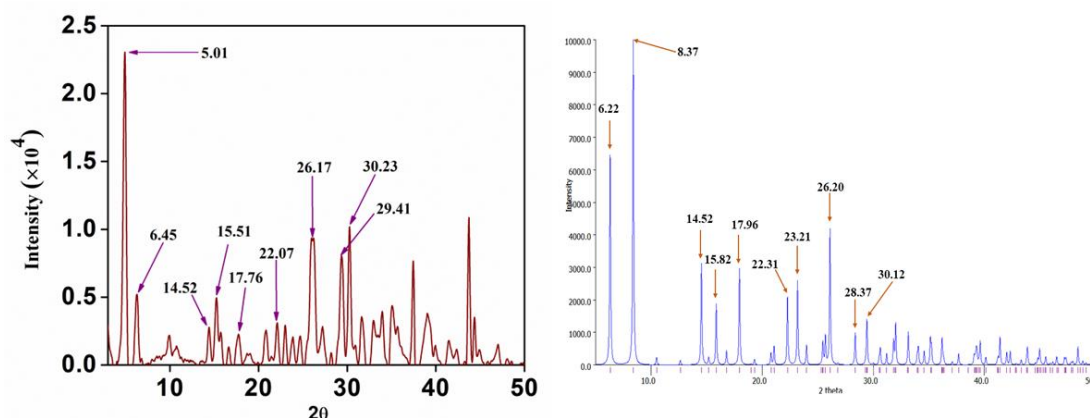

Figure 5.3: (a) Powder X-ray diffraction pattern of prepared K$_4$PTC; (b) Powder X-ray diffraction pattern of reported K$_4$PTC (CCDC Number: 1509483).

5.3.2. General Procedures for UV−Visible and Fluorescence Spectroscopy Studies

Due to the good solubility and optical properties of K$_4$PTC in water medium, the F$^-$ sensing experiment was performed in aqueous solution. A 10 mM stock solution of K$_4$PTC and AlCl$_3$ were prepared in ultra-pure water. Spectroscopy experiments were conducted with 2.5 mL of K$_4$PTC solution in water and subsequent addition of known amount of metal salts [1 × 10^{-2} M] at room temperature to monitor the change in optical properties of K$_4$PTC. The UV-Vis absorption experiments were performed with 10 μM aqueous solution of K$_4$PTC whereas corresponding fluorescence spectra were recorded with 1 μM aqueous solution in a quartz cuvette at an excitation wavelength of 465 nm at room temperature. Interference from other analytes were checked by introducing 1 mM solution of the ions

(Anion: F⁻, Cl⁻, Br⁻, I⁻, OH⁻, HSO₄⁻, H₂PO₄⁻, and CH₃COO⁻; Cation: Ca^{2+}, Ba^{2+}, Cu^{2+}, Fe^{2+}, Fe^{3+}, Ni^{2+}, V^{3+}, Zn^{2+}, Co^{2+}, Mn^{2+}, Mg^{2+}, Na^+, Al^{3+}) to each sample. The solutions of F⁻, Cl⁻, Br⁻, I⁻, OH⁻, HSO₄⁻, H₂PO₄⁻, and CH₃COO⁻ were prepared from their sodium salts. Recyclability experiments involved the alternate addition of 100 μL of 10 mM solution of Al^{3+} ion and 10 mM solution of NaF in a sequential manner.

5.3.3. Determination of F⁻ in Water Samples

Different volumes of standard solution of NaF (100 ppm) were added to prepare water samples containing different concentrations of F⁻ required to obtain the calibration plot. The methodology was validated with different concentration of NaF in ppm level prepared in tape water.

5.4. Results and Discussion

5.4.1. UV-Vis and Fluorescence study

K₄PTC is highly soluble in water, hence all the ion recognition experiment were performed in water medium. The ion screening experiment was done with done with UV-Vis and
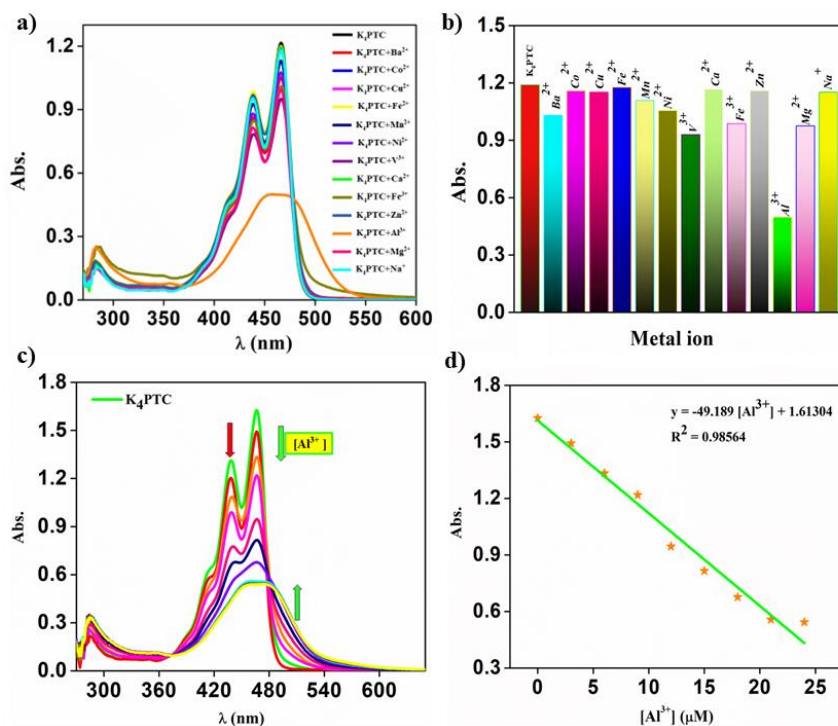
Figure 5.4: (a) UV−Vis absorption spectra of K₄PTC (10 μM) solution in water upon addition of 30μL different metal ions (10 mM); (b) Bar representation of the change in absorbance of the peak at 470 nm in presence of different metal ions; (c) Change in the UV−Vis absorption spectra of K₄PTC solution in water upon gradual addition of Al^{3+}; (d) change in absorbance of the peak at 470 nm with increase in the concentration of Al^{3+}.

fluorescence spectroscopy. The aqueous solution of K₄PTC solution showed two absorptions peaks at 438 and 470 nm. The metal ion binding study revealed that K₄PTC coordinated with Al^{3+} ion selectively among the tested metal ion (Figure 5.4 a,b). The UV-Vis spectra showed that the two absorption peaks of K₄PTC solution at 438 and 470 nm disappears upon addition of Al^{3+} and a new broad peak emerged at 480-530 leading to the colour change from greenish yellow to dark orange (Figure 5.4 c, 5.5c). The process became saturated upon addition of 60μL of 10mM of Al^{3+} aqueous solution (0.023 mM concentration of Al^{3+} in the reaction mixture). The UV-Vis titration data showed linear decrease of the absorbance of the peak at 470 nm upon incremental addition of concentration of the Al^{3+} in the medium. The Al^{3+} binding was further explored with fluorescence spectroscopy. The K₄PTC solution in water displayed two maxima at $\lambda_{em} = 485$ and 511 nm upon excitation at $\lambda_{exc} = 465$ nm. Like the observations in UV-Vis spectroscopy, addition of Al^{3+} (aq) solution to the K₄PTC solution in water showed gradual quenching of the fluorescence of K₄PTC solution and complete quenching of fluorescence
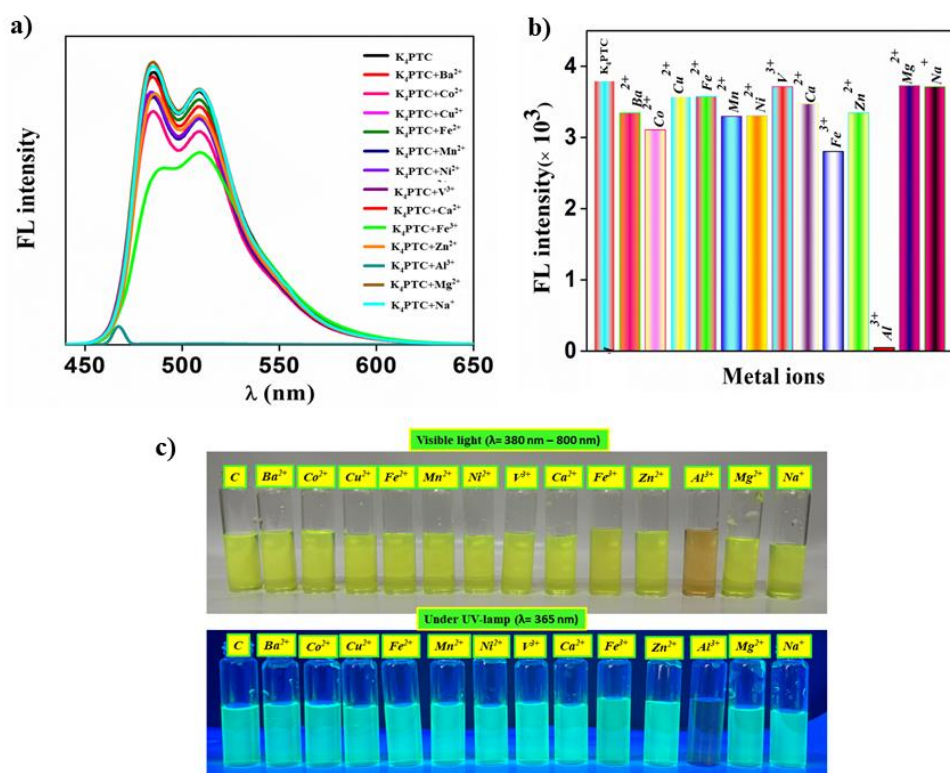

Figure 5.5: (a) UV−Vis absorption spectra of K₄PTC solution in water upon addition of different anions; (b) Bar representation of the change in absorbance at 465 nm upon addition of different anions to Al^{3+}-K₄PTC solution; (c) colorimetric and fluorometric changes. [**C= K₄PTC**].

was observed once the concentration of Al^{3+} in the reaction mixture reaches 0.023 mM (Figure 5.5a). As a consequence, the bright green fluorescence colour of the K_4PTC solution disappeared. However, other tested metal ions (Ca^{2+}, Ba^{2+}, Cu^{2+}, Fe^{2+}, Fe^{3+}, Ni^{2+}, V^{3+}, Zn^{2+}, Co^{2+}, Mn^{2+}, Mg^{2+}, and Na^+) did not have any impact on the fluorescence intensity of K_4PTC solution. These findings attributed to the formation of an *in-situ* Al^{3+}-PTC complex leading to the observed changes in the optical property of the solution. Furthermore, the titration of the K_4PTC solution with Al^{3+} ion was performed (Figure 5.6). The Stern-Volmer plot exhibited a non-linear behaviour which indicates that the quenching is static in nature. In other words, the complexation of Al^{3+} has taken place in ground state rather than in excited state (Figure 5.6b) [41,42]. From the plot of F_0/F vs $[Al^{3+}]$, the equilibrium constant for the Al^{3+}complexation reaction of K_4PTC (considering the linear variation up to 16 µM addition of F^-) was calculated and found as 1.06×10^3 M^{-1} [43].
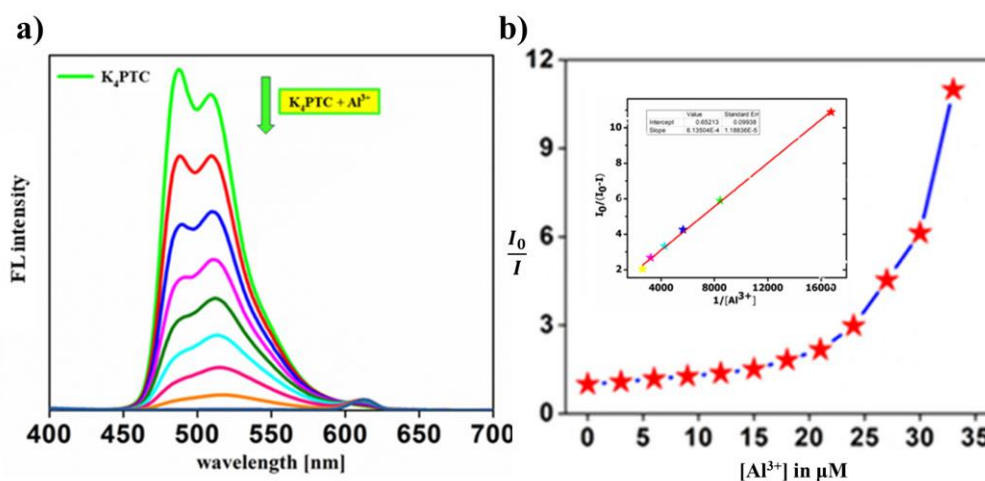

Figure 5.6: (a) Emission spectra of K_4PTC solution in water upon gradual addition of Al^{3+} ion to K_4PTC; (b) Stern-Volmer plot of quenching of emission of K_4PTC in presence of Al^{3+}.

The metal ion recognition study inferred that the K_4PTC selectively coordinated with Al^{3+} ion among the tested metal ions in water medium. Therefore, as per hypothesis 2 the affinity Al^{3+}-K_4PTC mixture in water towards the various anions was investigated. The UV-Vis titration study revealed that the peaks at 438 and 470 nm reappeared only after addition of F^- ion solution whereas other anions fail to do so (Figure 5.7a). The solution colour transformed from brownish red to greenish yellow as the original K_4PTC reappears in the reaction mixture (Figure 5.7c). Furtehrmore, fluorescence study also stated resurgence of the emission upon addition of NaF to the Al^{3+}-K_4PTC solution (Figure 5.8). These finding

attributed to the fact that F⁻ ion acted as Al³⁺ scavenger owing to the formation of stable $(AlF_x)^{(3-x)+}$ complex which eventually released the PTC^{4-} dye . Furthermore, UV-visible

Figure 5.7: (a) UV−Vis absorption spectra of K₄PTC solution in water upon addition of different anions; (b) Bar representation of the change in absorbance at 465 nm upon addition of different anions to Al³⁺-K₄PTC solution; (c) colorimetric and fluorometric changes. [**C= K₄PTC**].
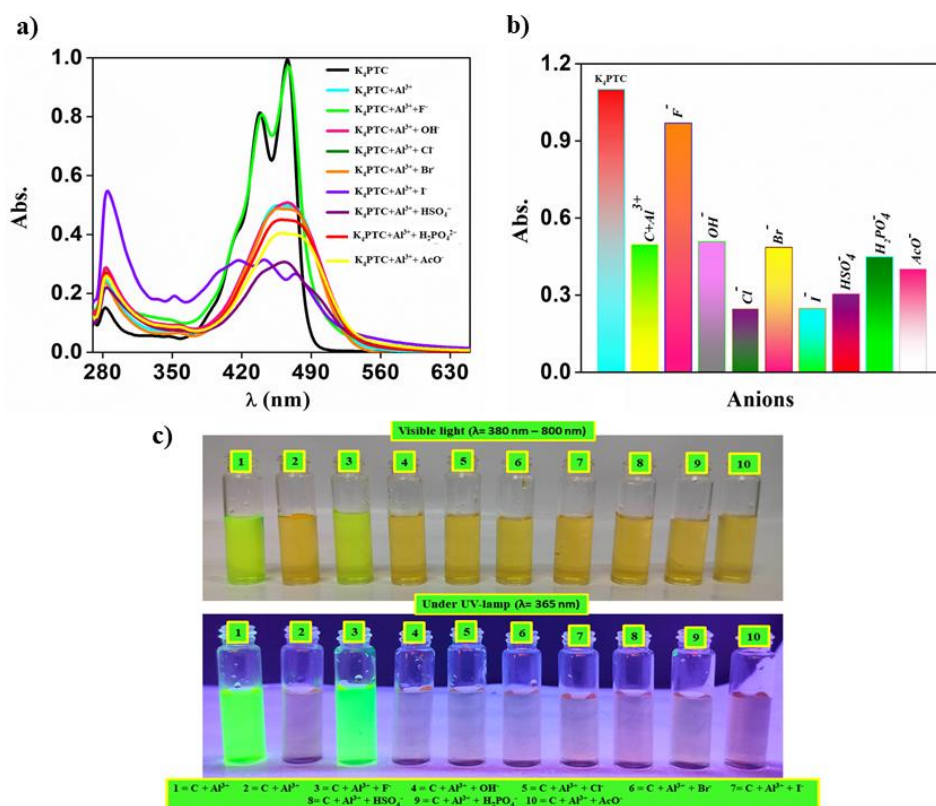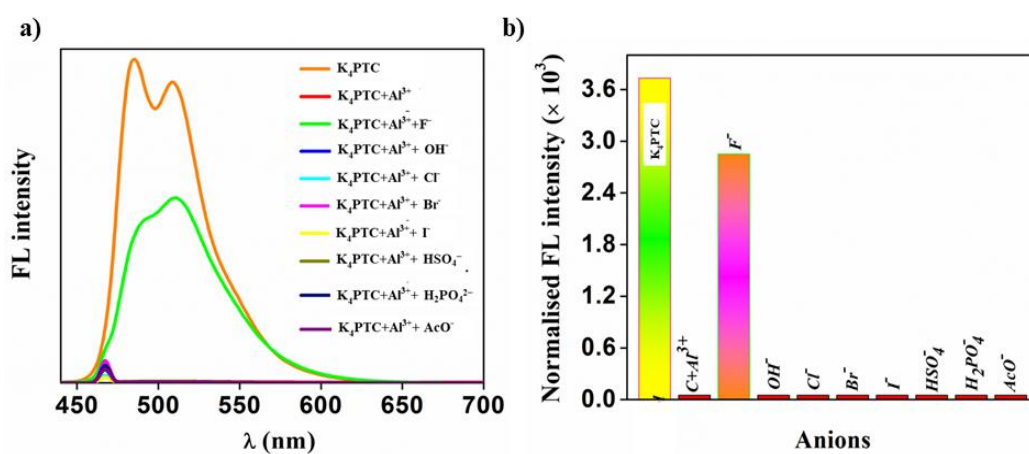

Figure 5.8: (a) Fluorescence spectra of K₄PTC solution in water upon addition of different metal ions; (b) Bar representation of the change in fluorescence intensity of 485 nm peak.
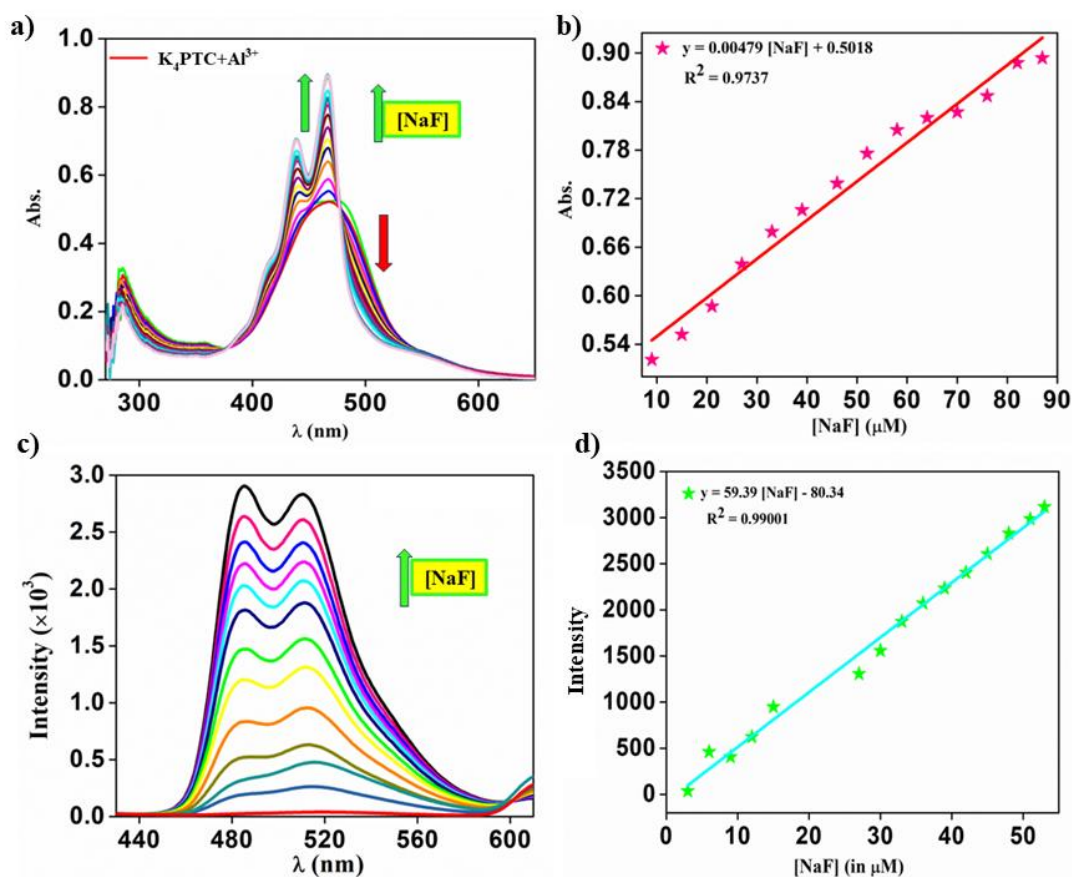
Figure 5.9: (a) UV-Vis absorption spectra of PTC- Al^{3+} solution upon gradual addition of F^- in water medium; (b) Change in absorbance of the peak at 470 nm of PTC- Al^{3+} mixture upon gradual addition of F^- in water medium; (c) Emission spectra of PTC- Al^{3+} upon gradual addition of F^- in water medium; (d) Increase in the intensity of emission at 511 nm of PTC- Al^{3+} mixture upon gradual addition of F^- in water medium.

titration study depicted that the broad peak at 457-478 nm disappeared with simultaneous increase in the absorbance of the peaks at 438 and 465 nm by following a ratiometric ($A_{\lambda=438}/A_{\lambda=503}$ and $A_{\lambda=465}/A_{\lambda=503}$) trend w.r.t. the concentration of F^- (Figure 5.9a). Similarly, fluorescence study also portrayed the gradual enhancement of the fluorescence intensity upon incremental addition of NaF solution (Figure 5.9c). Both the absorption and emission titration data revealed a linear variation with the added NaF concentration to the Al^{3+}-K_4PTC solution in water (Figure 5.9b,d).

The quantum yield of K_4PTC solution in water upon sequential addition of Al^{3+} and F^- ion is measured by considering Rhodamine B as reference [44,45]. Calculation of quantum yield of K_4PTC solution (1μM) revealed that upon addition of excess Al^{3+} ion the quantum

yield drops from 81% to 9.2%; however subsequent addition of excess F⁻ ion led to fluorescence turn on with the regain of the quantum yield upto 74 % (Figure 5.10). This observation confirmed that the dye, F⁻ can displace the PTC^{4-} dye from the Al^{3+}-PTC complex and the phenomena can be used in the development of fluorescent sensor for F⁻ ion in water medium with high contrast.
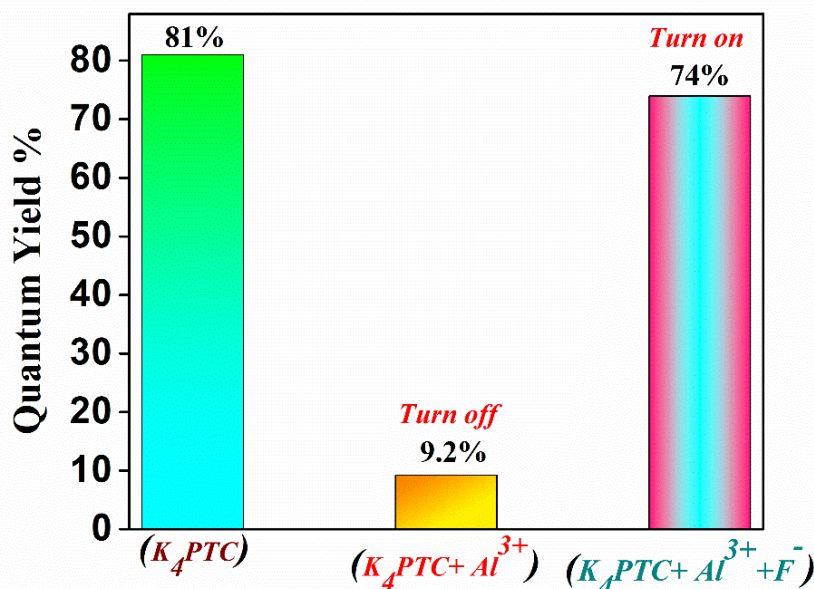

Figure 5.10: Change in the quantum yield of K_4PTC upon sequential addition of Al^{3+} and NaF in water.

To study the sensitivity of recognition of F⁻ ion by the in situ prepared PTC-Al^{3+} complex, increasing amount of F⁻ (aq) were added to the solution of PTC-Al^{3+} complex in water. The absorbance ratios ($A503/A438$ and $A503/A466$) against [F⁻] revealed a good linear relationship within the range from 0.2 to 8 ppm (10 to 526 µM) with a LOD of 0.2 ppm (0.59 µM) (R^2 = 0.98) (Figure 5.11). The LOD was calculated from the fluorescence intensities and found as 1 ppb (0.05 µM) (R^2 = 0.98), which is lower than that calculated from the UV-Vis spectroscopy. The low LODs implied that this bifunctional (colorimetric and fluorometric) approach for selective sensing of F⁻ ion in water medium with K_4PTC is suitable for monitoring F⁻ ion in drinking water.
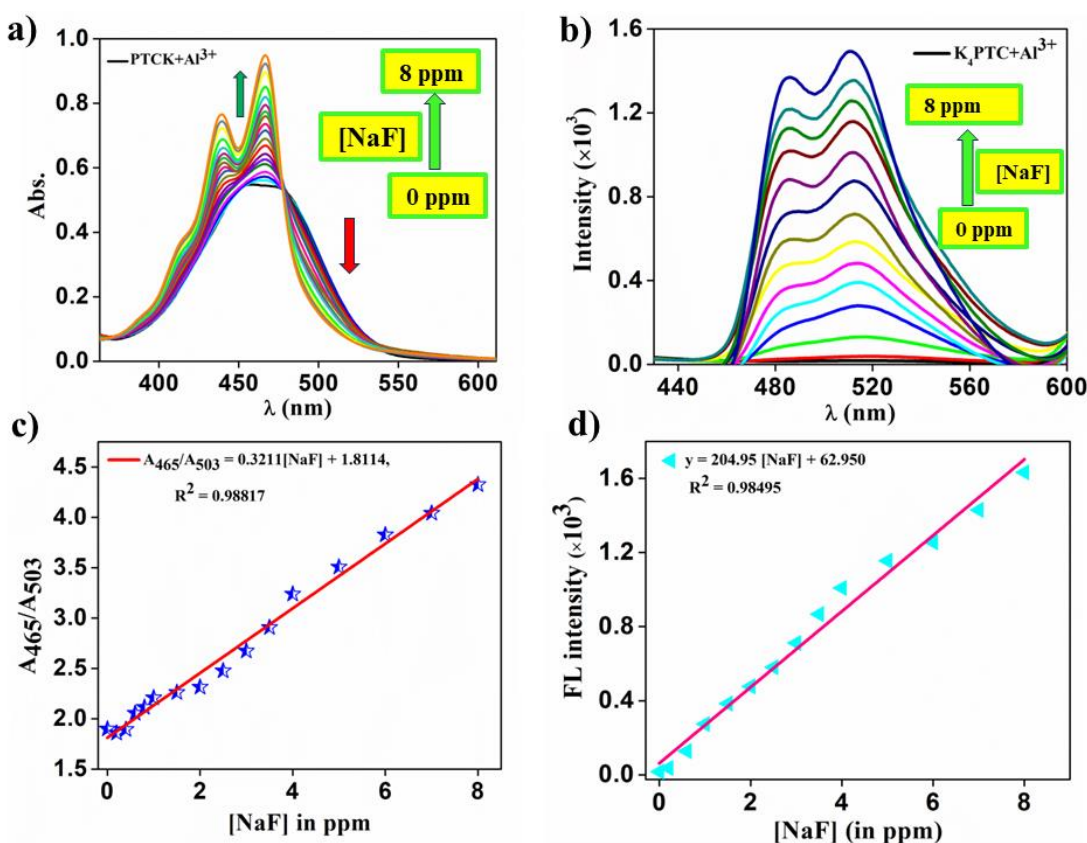
Figure 5.11: (a) Change in the absorbance of PTC-Al^{3+} mixture upon increasing amount of NaF (in ppm) in water; (b) Increase in the fluorescence intensity of PTC-Al^{3+} mixture upon increasing amount of NaF (in ppm) in water; (c) Linear variation of the ratio of absorbance at λ= 465 nm ad 503 nm upon increasing amount of NaF; (d) Linear variation of the emission intensity at λ= 511 nm upon increasing amount of NaF.

5.4.2. Recyclability Study

To test the reversibility of the sensing methodology, Al^{3+} was added to the aqueous solution having all the three components (K$_4$PTC, AlCl$_3$ and NaF) and the respective optical (absorption and emission) changes of the solution was monitored. The study revealed the emergence of the broad absorption peak at 457-478 nm and the quenching of the emission peak upon addition of Al^{3+} ion. Subsequent addition of F$^-$ ion to this solution led to disappearance of the UV-Vis peak at 457-478 nm associated with the fluorescence emission turn on at 510 nm. With the alternating addition of F$^-$ and Al^{3+}, the switching of absorbance and fluorescence was tested for five consecutive cycles and found good recyclability of the methodology (Figure 5.12).
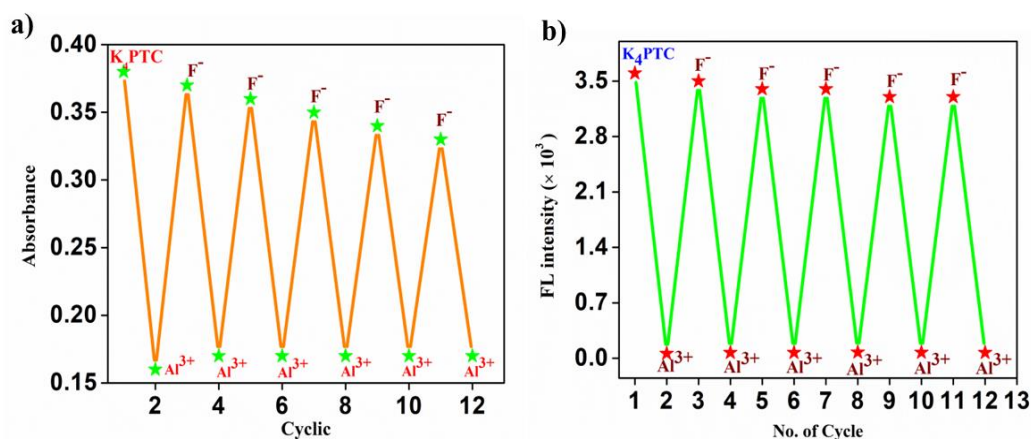
Figure 5.12: Recyclability of the probe characterized by (a) UV−vis absorption spectroscopy and (b) fluorescence spectra.

5.4.3. Investigation of the sensing mechanism

As a hard metal ion Al^{3+} (aq) forms stable complexes with strong hard bases like F^- ion [46,47]. Carboxylate oxygens are relatively less hard than F^-, therefore it was presumed that F^- can easily take out Al^{3+} that forms complex with perylelene tetracarboxylate (PTC) ligand and form stable $(AlF_x)^{(3-x)+}$(aq) complex. The complexation of Al^{3+} with PTC^{4-} led to substantial changes in the absorption as well as quenching of emission. However, the average life time (from TRPL study) of the excited state K_4PTC did not vary (5.2×10^{-9} s and 5.4×10^{-9} s in absence and presence of Al^{3+} respectively) indicating the complexation at the ground state rather than the excited state, pointing to the static nature of quenching (Figure 5.13 a,b) [48,49]. The Stern-Volmer plot also exhibited a non-linear behaviour which further conferred the static quenching of Fluorescence of K_4PTC by Al^{3+}. However, upon subsequent addition of F^-, the fluorescence gets turn on suggesting removal of Al^{3+} ion by F^- ion owing to the formation of Al^{3+}-fluoride complex. The average life time of the solution containing all the three components was found as 5.2×10^{-9} s similar to the K_4PTC solution. To validate the formation of the Al^{3+}-fluoride complex, the K_4PTC, Al^{3+} and F^- mixture in water was precipitated out by adding ethanol and the precipitate was dried and analysed. FTIR analysis showed the peak at 600 cm^{-1} attributing to the vibrational stretching frequency of F-Al-F species (Figure 5.13c) [50]. Furthermore, we have carried out the reaction of K_4PTC, Al^{3+} and F^- in D_2O and recorded the ^{19}F spectra. The ^{19}F spectra showed the peak at -156.1 ppm which also dictated the formation of $(AlF_x)^{(3-x)+}$ species in

the reaction mixture (Figure 5.13d) [51]. The plausible mechanism involved in the sensing process is depicted in figure 5.14.

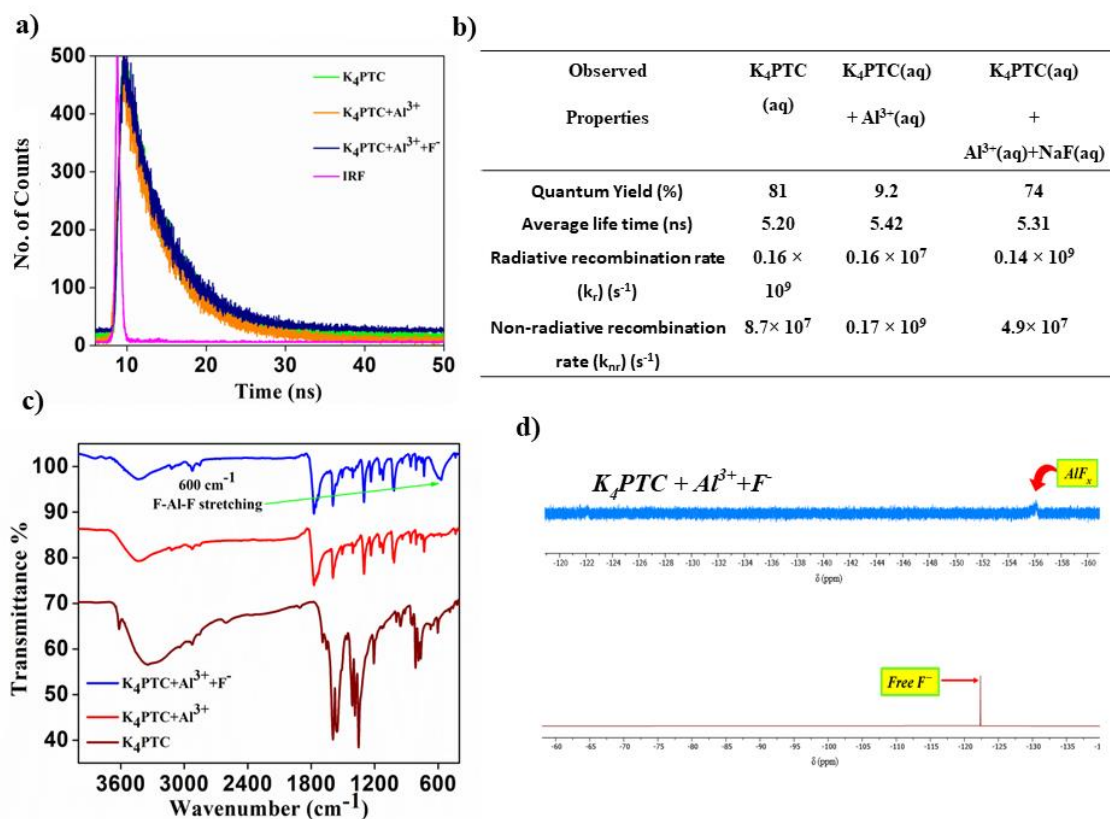**Figure 5.13:** (a) Time resolved photoluminescence spectra of K_4PTC in presence of Al^{3+} and F^-; (b) Table representation of the decay rates; (c) FTIR spectra of K_4PTC and K_4PTC in presence of Al^{3+} and F; (d) ^{19}F NMR spectra: top- K_4PTC, Al^{3+} and F^- mixture in D_2O; bottom: K_4PTC and F^- mixture in D_2O.
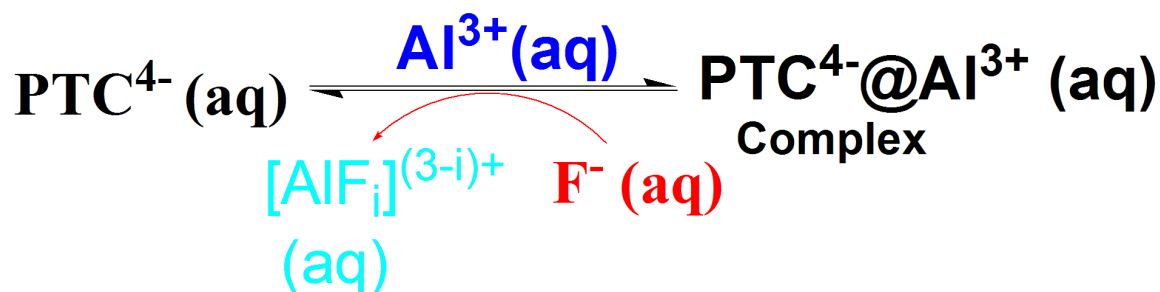

Figure 5.14: Plausible reactions involved in the sensing process

5.5. Validation of the method with real life sample

In order to check the applicability of the methodology towards detection of fluoride ion in water, we have checked our methodology's performance with F$^-$ contaminated laboratory samples and samples collected from the Karbi Anglong district of Assam, India. For the UV-Vis analysis, 2.5 mL of a 1.6×10^{-4} M solution of K$_4$PTC was placed in a cuvette, and 70 μL of a 10×10^{-3} M AlCl$_3$ solution in aqueous medium was added. Subsequently, 50 μL of each water sample was added separately to each mixture. For fluorescence measurement, 2.5 mL of 1.2×10^{-5} M solution of K$_4$PTC was placed in a cuvette, and 70 μL of a 1×10^{-3} M AlCl$_3$ solution in an aqueous medium was added. Then, 50 μL of water having known concentration of fluoride was added separately to each mixture and the optical change was monitored with UV-Vis as well as the fluorescence spectrometer. From the data, the linear calibration curve was obtained (Figure 5.11 c,d). Subsequently, the absorption and emission behaviour of the K$_4$PTC-Al^{3+} solution was measured upon addition of the water sample having unknown fluoride concentration. The solution exhibited the characteristic colorimetric and fluorometric change regaining the orange-red colour and greenish-yellow fluorescence, indicative of the presence of fluoride ion (Figure 5.15). The fluoride ion

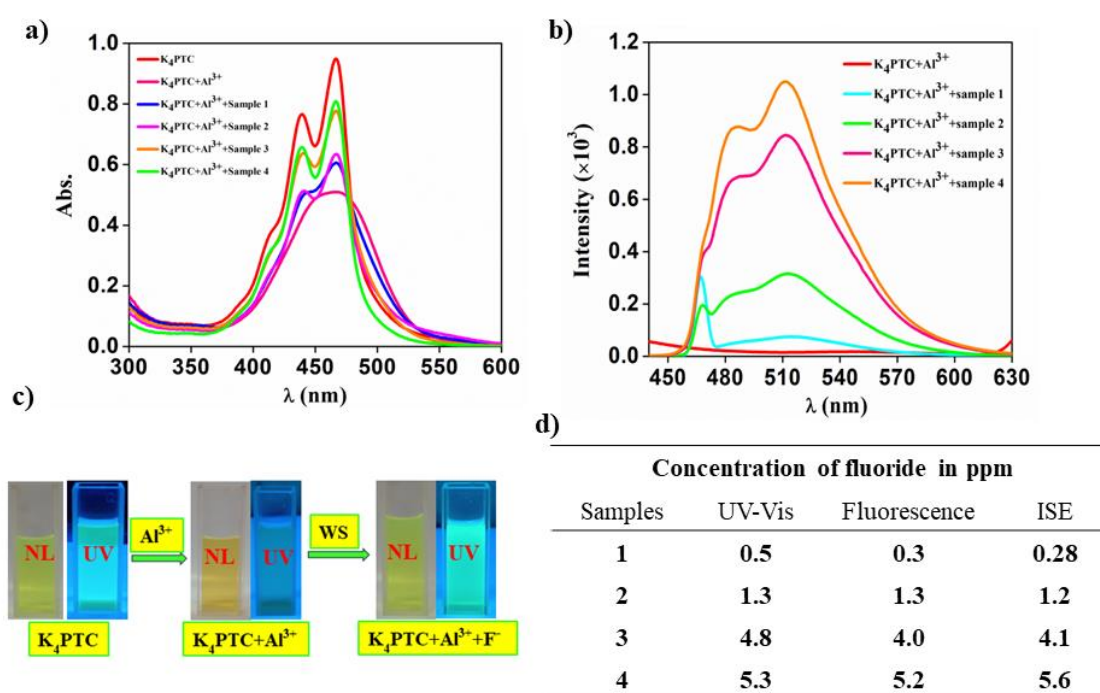| Samples	UV-Vis	Fluorescence	ISE
1	0.5	0.3	0.28
2	1.3	1.3	1.2
3	4.8	4.0	4.1
4	5.3	5.2	5.6

Figure 5.15: Measurement of the concentration of fluoride in the water sample (a) UV-Vis spectra, (b) emission spectra, (c) change in colour of the solution upon addition of water sample; (d) comparison of the fluoride data with ion selective electrode (ISE) data.

concentration was determined from the calibration curve, producing a value as shown in Table incorporated in the figure 5.15d for laboratory prepared samples and sample collected from Karbianglong district of Assam, India. The results were found to be in good agreement with those obtained from ion-selective electrode (ISE) measurements. The deviation between the methodology and the ISE measurement could be attributed to experimental errors. This study underscores the capability of this dye displacement methodology to assess the presence of fluoride ions in both qualitative and quantitative aqueous media.

5.6. Conclusion

A perylene tetracarboxylate dye-based MOF (K_4PTC) is demonstrated as a fluorometric as well as colorimetric probe for sensing of F^- ion in 100% water. K_4PTC shows turn off fluorescence response in presence of Al^{3+} ions. However, subsequent addition of fluoridated water results naked eye discernible fluorescence turns on response. The LOD value calculated for F^- ion was found to be 0.2 ppm and 1 ppb for UV-Vis and Fluorometric technique respectively. The detection range is found to be within the concentration limit set as per WHO guideline for fluoride ion. The chemosensor can be easily recyclable for further application with good performance up to fifth cycle. The present work highlights a simple method for rapid and sensitive detection of fluoride in water with high precision with the aid of a common organic fluorescent dye, 3,4,9,10-Perylenetetracarboxylate.

5.7. References

[1]   Kardos M., Deutsches Reichspatent, Vol. 276357, 1913.

[2]   Li, C., and Wonneberger, H. Perylene imides for organic photovoltaics: yesterday, today, and tomorrow. *Advanced Materials*, 24(5):613-636, 2012.

[3]   Golshan, M., Rostami-Tapeh-Esmail, E., Salami-Kalajahi, M., and Roghani-Mamaqani, H. A review on synthesis, photophysical properties, and applications of dendrimers with perylene core. *European Polymer Journal*, 137:109933, 2020.

[4]   Nagao, Y. Synthesis and properties of perylene pigments. *Progress in organic coatings*, 31(1-2):43-49, 1997.

[5]   Chai, S., Wen, S. H., and Han, K. L. Understanding electron-withdrawing substituent effect on structural, electronic and charge transport properties of perylene bisimide derivatives. *Organic electronics*, 12(11):1806-1814, 2011.

[6]   Maia, P. J. S., Cruz, J. F., de Freitas, F. A., de Fátima Freire dos Santos, S., and de Souza, E. A. Photophysical properties of a perylene derivative for use as catalyst in ethanol eletrooxidation. *Research on Chemical Intermediates*, 45:5451-5472, 2019.

[7]   Li, C., and Wonneberger, H. Perylene imides for organic photovoltaics: yesterday, today, and tomorrow. *Advanced Materials*, 24(5):613-636, 2012.

[8]   Chen, S., Slattum, P., Wang, C., and Zang, L. Self-assembly of perylene imide molecules into 1D nanostructures: methods, morphologies, and applications. *Chemical reviews*, 115(21):11967-11998, 2015.

[9]   Singh, P., Kumar, K., Bhargava, G., and Kumar, S. Self-assembled nanorods of bay functionalized perylenediimide: Cu^{2+} based 'turn-on'response for INH complementary NOR/OR and TRANSFER logic functions and fluorosolvatochromism. *Journal of Materials Chemistry C*, 4(13):2488-2497, 2016.

[10]   Kundu, A.; Pitchaimani, J.; Madhu, V.; Sakthive, P.; Ganesamoorthy, R., and Anthony, S.P. Bay Functionalized Perylenediimide with Pyridine Positional Isomers: NIR Absorption and Selective Colorimetric/Fluorescent Sensing of Fe^{3+} and Al^{3+} Ions. J. Fluoresc. 27, 491–500, 2017.

[11]   Du, F., Bao, Y., Liu, B., Tian, J., Li, Q., and Bai, R. POSS-containing red fluorescent nanoparticles for rapid detection of aqueous fluoride ions. *Chemical Communications*, 49(41): 4631-4633, 2013.

[12]   Ajayakumar, M. R., Mukhopadhyay, P., Yadav, S., and Ghosh, S. Single-electron transfer driven cyanide sensing: a new multimodal approach. *Organic Letters*, 12(11):2646-2649, 2010.

[13]   Dey, S., and Sukul, P. K. Selective detection of pyrophosphate anions in aqueous medium using aggregation of perylene diimide as a fluorescent probe. *ACS omega*, 4(14):16191-16200, 2019.

[14]   Zhang, L., Wang, L., Zhang, G., Yu, J., Cai, X., Teng, M., and Wu, Y. A Highly Sensitive and Selective Colorimetric Chemosensor for F^- Detection Based on Perylene-3, 4: 9, 10-tetracarboxylic Bisimide. *Chinese Journal of Chemistry*, 30(12):2823-2826, 2012.

[15] Wang, Y., Zhang, L., Zhang, G., Wu, Y., Wu, S., Yu, J., and Wang, L. A new colorimetric and fluorescent bifunctional probe for Cu^{2+} and F^- ions based on perylene bisimide derivatives. *Tetrahedron Letters*, 55(21):3218-3222, 2014.

[16] Shibano, Y., Imahori, H., and Adachi, C. Organic thin-film solar cells using electron-donating perylene tetracarboxylic acid derivatives. *The Journal of Physical Chemistry C*, 113(34):15454-15466, 2009.

[17] Suresh, D. S., Vijaykumar, S. P., Sharanappa, S., Shbil, A. B., Ganesha, H., Veeresh, S., and Devendrappa, H. Novel approach towards optically active and hexagonal plate morphology of Zinc doped Perylene Tetra Carboxylic Di Anhydride composite for high photovoltaic and flexible supercapacitor performances. *Journal of Power Sources*, 593:233967, 2024.

[18] Valente, G., Esteve-Rochina, M., Alves, S. P., Martinho, J. M., Ortí, E., Calbo, J., and Souto, M. Perylene-Based Coordination Polymers: Synthesis, Fluorescent J-Aggregates, and Electrochemical Properties. *Inorganic Chemistry*, 62(20):7834-7842, 2023.

[19] Gao, X., Liu, Z., Tuo, X., Chen, S., Cai, S., Yan, M., and Liu, Z. A case study on storage and capacity fading mechanism of poly (perylene diimides) cathode in aqueous zinc ion battery. *Electrochimica Acta*, 453:142321, 2023.

[20] Zhou, W., Liu, G., Yang, B., Ji, Q., Xiang, W., He, H., and Xu, C. Review on application of perylene diimide (PDI)-based materials in environment: Pollutant detection and degradation. *Science of The Total Environment*, 780:146483, 2021.

[21] He, X. R., Liu, H. B., Li, Y. L., Wang, S., Li, Y. J., Wang, N., and Zhu, D. B. Gold nanoparticle-based fluorometric and colorimetric sensing of copper (II) ions, 2005.

[22] Guha, S., Goodson, F. S., Roy, S., Corson, L. J., Gravenmier, C. A., and Saha, S. Electronically regulated thermally and light-gated electron transfer from anions to naphthalenediimides. *Journal of the American Chemical Society*, 133(39):15256-15259, 2011.

[23] Guha, S., Goodson, F. S., Corson, L. J., and Saha, S. Boundaries of anion/naphthalenediimide interactions: from anion−π interactions to anion-induced

charge-transfer and electron-transfer phenomena. *Journal of the American Chemical Society*, 134(33):13679-13691, 2012.

[24] Goodson, F. S., Panda, D. K., Ray, S., Mitra, A., Guha, S., and Saha, S. Tunable electronic interactions between anions and perylenediimide. *Organic & Biomolecular Chemistry*, 11(29):4797-4803, 2013.

[25] Saha, S. Anion-induced electron transfer. *Accounts of Chemical Research*, 51(9): 2225-2236, 2018.

[26] Dwivedi, A. K., Pandeeswar, M., and Govindaraju, T. Assembly modulation of PDI derivative as a supramolecular fluorescence switching probe for detection of cationic surfactant and metal ions in aqueous media. *ACS Applied Materials & Interfaces*, 6(23):21369-21379, 2014.

[27] Chen, S., Xue, Z., Gao, N., Yang, X., and Zang, L. Perylene diimide-based fluorescent and colorimetric sensors for environmental detection. *Sensors*, 20(3):917, 2020.

[28] Mu, M., Ke, X., Cheng, W., Li, J., Ji, C., and Yin, M. Perylenemonoimide-based colorimetric probe with high contrast for naked-eye detection of fluoride ions. *Analytical Chemistry*, 94(33):11470-11475, 2022.

[29] Lu, J., Sun, R., Chen, M., Xu, X., and Zhang, X. Design, synthesis, and self-assembly of optically active perylenetetracarboxylic diimide bearing two peripheral chiral binaphthyl moieties. *Materials Science and Engineering: C*, 32(7):1948-1954, 2012.

[30] Rostami-Tapeh-Esmail, E., Golshan, M., Salami-Kalajahi, M., and Roghani-Mamaqani, H. Perylene-3, 4, 9, 10-tetracarboxylic diimide and its derivatives: Synthesis, properties and bioapplications. *Dyes and Pigments*, 180:108488, 202.

[31] Zhang, M., Liang, R., Li, K., Chen, T., Li, S., Zhang, Y., and Chen, X. Dual-emitting metal–organic frameworks for ratiometric fluorescence detection of fluoride and Al^{3+} in sequence. *Spectrochimica Acta Part A: Molecular and Biomolecular Spectroscopy*, 271:120896, 2022.

[32] Chen, Y., Luo, W., Carter, M., Zhou, L., Dai, J., Fu, K., and Hu, L. Organic electrode for non-aqueous potassium-ion batteries. *Nano Energy*, 18:205-211, 2015.

[33] Seco Botana, J. M., San Sebastián Larzabal, E., Cepeda Ruiz, J., Biel, B., Salinas-Castillo, A., Fernández, B., and Rodríguez-Diéguez, A. A Potassium Metal-Organic

Framework based on Perylene-3, 4, 9, 10-tetracarboxylate as Sensing Layer for Humidity Actuators, 2018.

[34] Rajamohan, R., Rubyraj, M., Selvamani, T., Krishnan, M. M., Govindasamy, C., Murugan, M., and Lee, Y. R. Chemosensor material as a metal–organic framework with potassium-based perylene tetracarboxylic acid for copper and lead detection. *Journal of Molecular Liquids*, 125376, 2024.

[35] Mu, M., Ke, X., Cheng, W., Li, J., Ji, C., and Yin, M. Perylenemonoimide-based colorimetric probe with high contrast for naked-eye detection of fluoride ions. *Analytical Chemistry*, 94(33):11470-11475, 2022.

[36] Wang, R., Li, J., Li, G., Hao, C., Zhang, Y., Wang, S., and Shi, Z. Synthesis of 1-amino-12-hydroxyl-perylene tetra-(alkoxycarbonyl) for selective sensing of fluoride. *Dyes and Pigments*, 156:225-232, 2018.

[37] Chen, Z. J., Wang, L. M., Zou, G., Zhang, L., Zhang, G. J., Cai, X. F., and Teng, M. S. Colorimetric and ratiometric fluorescent chemosensor for fluoride ion based on perylene diimide derivatives. *Dyes and Pigments*, 94(3):410-415, 2012.

[38] Maiti, D. K., Roy, S., Datta, A., and Banerjee, A. Aqueous fluoride ion sensing by a new perylenediimide derivative: Interaction between the hydrated fluoride and the aromatic molecule. *Chemical Physics Letters*, 588:76-81, 2013.

[39] Wang, Y.F., Zhang, L., Zhang, G.J., Wu, Y., Wu, S.Y., and Yu, J.J. A new colorimetric and fluorescent bifunctional probe for Cu^{2+} and F^- ions based on perylene bisimide derivatives. *Tetrahedron Lett.* 55:3218–3222, 2014.

[40] Chen, Y., Luo, W., Carter, M., Zhou, L., Dai, J., Fu, K., and Hu, L. Organic electrode for non-aqueous potassium-ion batteries. *Nano Energy*, 18:205-211, 2015.

[41] Keizer, J. Nonlinear fluorescence quenching and the origin of positive curvature in Stern-Volmer plots. *Journal of the American Chemical Society*, 105(6):1494-1498, 1983.

[42] Gehlen, M. H. The centenary of the Stern-Volmer equation of fluorescence quenching: From the single line plot to the SV quenching map. *Journal of Photochemistry and Photobiology C: Photochemistry Reviews*, 42:100338, 2020.

[43] Van de Weert, M., and Stella, L. Fluorescence quenching and ligand binding: A critical discussion of a popular methodology. *Journal of Molecular Structure*, 998(1-3):144-150, 2011.

[44] Bindhu, C. V., Harilal, S. S., Varier, G. K., Issac, R. C., Nampoori, V. P. N., and Vallabhan, C. P. G. (1996). Measurement of the absolute fluorescence quantum yield of rhodamine B solution using a dual-beam thermal lens technique. *Journal of Physics D: Applied Physics*, 29(4):1074, 1996.

[45] Brouwer, A.M. Standards for photoluminescence quantum yield measurements in solution. *Pure and Applied Chemistry* 83(12):2213-2228, 2011.

[46] Pearson, R. G. Hard and soft acids and bases. *Journal of the American Chemical society*, 85(22):3533-3539, 1963.

[47] Pearson, R. G., and Songstad, J. Application of the principle of hard and soft acids and bases to organic chemistry. *Journal of the American Chemical Society*, 89(8):1827-1836, 1967.

[48] Pal, A., Srivastava, S., Saini, P., Raina, S., Ingole, P. P., Gupta, R., and Sapra, S. Probing the mechanism of fluorescence quenching of QDs by Co (III)-Complexes: size of QD and nature of the complex both dictate energy and electron transfer processes. *The Journal of Physical Chemistry C*, 119(39):22690-22699, 2015.

[49] Baranowski, M., Urban, J. M., Zhang, N., Surrente, A., Maude, D. K., Andaji-Garmaroudi, Z., and Plochocka, P. Static and dynamic disorder in triple-cation hybrid perovskites. *The Journal of Physical Chemistry C*, 122(30):17473-17480, 2018.

[50] König, R., Scholz, G., Scheurell, K., Heidemann, D., Buchem, I., Unger, W. E. S., and Kemnitz, E. Spectroscopic characterization of crystalline AlF_3 phases. *Journal of fluorine chemistry*, 131(1):91-97, 2010.

[51] Jin, Y., Molt Jr, R. W., Pellegrini, E., Cliff, M. J., Bowler, M. W., Richards, N. G., and Waltho, J. P. Assessing the Influence of Mutation on GTPase Transition States by Using X-ray Crystallography, ^{19}F NMR, and DFT Approaches. *Angewandte Chemie International Edition*, 56(33):9732-9735, 2017.